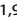

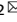


ARTICLE



Surfactant protein D inhibits lipid-laden foamy macrophages and lung inflammation in chronic obstructive pulmonary disease

Miao-Hsi Hsieh^{1,2}, Pei-Chi Chen^{1,3}, Han-Yin Hsu⁴, Jui-Chang Liu⁴, Yu-Sheng Ho⁴, Yuh Jyh Lin⁵, Chin-Wei Kuo^{6,7}, Wen-Shuo Kuo^{1,8}, Hui-Fang Kao³, Shulhn-Der Wang^{1,9}, Zhi-Gang Liu¹⁰, Lawrence Shih-Hsin Wu^{1,11}  and Jiu-Yao Wang ^{1,12} 

© The Author(s), under exclusive licence to CSI and USTC 2022

Increased levels of surfactant protein D (SP-D) and lipid-laden foamy macrophages (FMs) are frequently found under oxidative stress conditions and/or in patients with chronic obstructive pulmonary disease (COPD) who are also chronically exposed to cigarette smoke (CS). However, the roles and molecular mechanisms of SP-D and FMs in COPD have not yet been determined. In this study, increased levels of SP-D were found in the bronchoalveolar lavage fluid (BALF) and sera of ozone- and CS-exposed mice. Furthermore, SP-D-knockout mice showed increased lipid-laden FMs and airway inflammation caused by ozone and CS exposure, similar to that exhibited by our study cohort of chronic smokers and COPD patients. We also showed that an exogenous recombinant fragment of human SP-D (rfhSP-D) prevented the formation of oxidized low-density lipoprotein (oxLDL)-induced FMs in vitro and reversed the airway inflammation and emphysematous changes caused by oxidative stress and CS exposure in vivo. SP-D upregulated bone marrow-derived macrophage (BMDM) expression of genes involved in countering the oxidative stress and lipid metabolism perturbations induced by CS and oxLDL. Our study demonstrates the crucial roles of SP-D in the lipid homeostasis of dysfunctional alveolar macrophages caused by ozone and CS exposure in experimental mouse emphysema, which may provide a novel opportunity for the clinical application of SP-D in patients with COPD.

Keywords: Alveolar macrophages; Chronic obstructive pulmonary diseases; Surfactant protein D; Lipid metabolism; Ozone; Cigarettes

Cellular & Molecular Immunology (2023) 20:38–50; <https://doi.org/10.1038/s41423-022-00946-2>

INTRODUCTION

Chronic obstructive pulmonary disease (COPD) is a serious lung disease that has exhibited increasing morbidity and mortality worldwide [1]. It is the seventh leading cause of death in Taiwan [2] and third in the United States [3]. Although the underlying pathogenic mechanism of COPD remains unclear, inhaled oxidants such as cigarette smoke (CS) and air pollution dysregulate the expression of proteolytic enzymes and reactive oxygen species (ROS) that contribute to the production of inflammatory mediators and the release of metalloproteases from alveolar macrophages (AMs) to damage alveolar structure [4]. Existing therapeutic approaches are largely ineffective against the progressive deterioration of lung function and mortality in

COPD [1]. Thus, it is imperative to clarify the underlying mechanisms and develop targeted therapies for treating patients with COPD.

Surfactant protein-D (SP-D) is a hydrophilic lung surfactant protein secreted by alveolar type II cells and recycled by AMs [5]. SP-D plays a significant role in the protection against COPD by reducing the production of oxidants [6] and inflammatory responses in AMs [7] and increasing apoptotic cell clearance [8]. Increased oxidant and ROS production have been noted in the lungs of SP-D^{-/-} mice [9]. Mice that lack SP-D develop chronic inflammation and emphysema, which can be prevented by the administration of truncated recombinant human SP-D [6]. AMs from SP-D-deficient mice exhibit increased lipid accumulation and

¹Center for Allergy, Immunology, and Microbiome (A.I.M.), China Medical University Hospital, Taichung, Taiwan, China. ²Graduate Institute of Basic Medical Sciences, College of Medicine, National Cheng Kung University, Tainan, Taiwan, China. ³Department of Nursing, National Tainan Junior College of Nursing, Tainan, Taiwan, China. ⁴Graduate Institute of Biochemistry and Molecular Biology, College of Medicine, National Cheng Kung University, Tainan, Taiwan, China. ⁵Department of Pediatrics, National Cheng Kung University Hospital, Tainan, Taiwan, China. ⁶Division of Pulmonary Medicine, Department of Internal Medicine, National Cheng Kung University Hospital, College of Medicine, National Cheng Kung University, Tainan, Taiwan, China. ⁷Institute of Clinical Medicine, College of Medicine, National Cheng Kung University, Tainan, Taiwan, China. ⁸School of Chemistry and Materials Science, Nanjing University of Information Science and Technology, Nanjing, China. ⁹School of Post-Baccalaureate Chinese Medicine, China Medical University, Taichung, Taiwan, China. ¹⁰Department of Respiriology and Allergy, Third Affiliated Hospital of Shenzhen University, Shenzhen, China. ¹¹Institute of Biomedical Sciences, China Medical University, Taichung, Taiwan, China. ¹²Department of Allergy, Immunology, and Rheumatology (AIR), China Medical University Children's Hospital, Taichung, Taiwan, China. email: lshwu@hotmail.com; a122@mail.ncku.edu.tw

Received: 22 July 2022 Accepted: 27 October 2022

Published online: 14 November 2022

matrix metalloproteinase (MMP) and inflammatory cytokine production. These lipid-laden foamy macrophages (FMs), which are activated by oxidative stress and exposure to cigarette smoke (CS), have been observed in COPD, other pulmonary disorders, and SP-D deficient mice [10, 11]. High levels of ROS induce LDL oxidation and promote the differentiation of FMs in SP-D-deficient mice [12, 13]. Lysosomal acid lipase deficiency results in the accumulation of foamy AMs, which also contain excess cholesterol ester, resulting in emphysema in the aged lung [14]. Thus, foamy AMs may be involved in the development of various lung diseases, including emphysema.

A recent systematic review and meta-analysis confirmed the significant contribution of SP-D in patients with COPD and suggested that serum SP-D levels could serve as a potential biomarker of COPD [15]. Higher serum SP-D levels are associated with COPD risk [16]. Serum SP-D levels were higher in smokers than in nonsmokers in a healthy population. These levels are significantly higher in COPD patients. However, there was a difference in the serum SP-D levels of patients with acute COPD exacerbation and those of stable patients [17]. The correlation between the increased serum SP-D levels and COPD severity may involve the leakage of alveolar SP-D across the inflamed or damaged alveolar-capillary membrane [16]. Moreover, the increased serum SP-D levels in patients with COPD can be reduced by treatment with anti-inflammatory glucocorticoids, which highlights the potential role of SP-D as a biomarker for acute COPD inflammation [16]. Using a large cohort of patients with COPD, Obeidat et al. [18] investigated the association between genetic variations and SP-D protein levels, gene expression, and disease phenotypes based on Mendelian randomization. They established a causal link between increased SP-D levels and protection against COPD risk and progression [18]. We also demonstrated that genetic variants of SP-D are not only associated with the risk of COPD development but are also related to disease manifestations and long-term outcomes in our cohort population [19]. Thus, SP-D is not only a potential biomarker but also a potential therapeutic target for COPD.

To elucidate the role of SP-D and its interaction with lipid-laden FMs in COPD, wild-type C57BL/6 and SP-D^{-/-} mice were chronically exposed to ozone or CS to induce airway inflammation and emphysematous changes representative of the clinical features of COPD. Using a mouse model of COPD, we found that exogenous administration of a recombinant fragment of human SP-D (rhSP-D) prevents the formation of FMs by regulating lipid metabolism, thereby protecting against airway inflammation and alveolar emphysematous changes.

RESULTS

Increased SP-D expression in mice with ozone-induced COPD

We evaluated SP-D levels in a mouse model of COPD. The mice were subjected to chronic ozone exposure that directly destroyed alveolar structure and induced airway inflammation, resulting in chronic lung disease. After 3 weeks of ozone or air exposure, the mice were administered increasing doses of methacholine. In ozone-exposed mice, 1 and 3 ppm ozone increased respiratory system elastance (Ers) and lung tissue damping (G), while 3 ppm ozone also significantly increased respiratory-flow resistance (Rrs) and lung-tissue elastance (H) compared to those in air-exposed mice (Fig. 1A). Lung histology showed severe bronchial inflammation and alveolar space enlargement in ozone-exposed mice but not in control mice (Fig. 1B). Ozone increased the mean linear intercept (MLI) in a dose-dependent manner (Fig. 1C). Ozone exposure not only increased total inflammatory cell infiltration in the lung, particularly that of macrophages and neutrophils (Fig. 1D), but also promoted the secretion of TNF- α , IL-6, and CXCL1 in bronchoalveolar lavage fluid (BALF) (Fig. 1E). These results indicate that chronic exposure to 3 ppm ozone for 3 weeks

successfully induced airway inflammation and alveolar emphysema in mice, and the levels of SP-D in the serum and BALF were significantly increased in ozone-exposed mice (Fig. 1F).

Increased SP-D expression in mice with CS-induced COPD

We evaluated the SP-D levels in a mouse model of CS-induced COPD, which is comparable to the etiologic inducer of COPD in human. The mice were exposed to the smoke of 6 burning cigarettes for 1 h, 5 times per week for 6 weeks (Fig. S1A). CS exposure significantly increased the Rrs, Ers, and G after 200 mg/mL methacholine challenge compared to those in control mice exposed to air (Fig. S1B). Lung histological sections (H&E staining) showed that CS exposure increased mucus production in the bronchioles and caused emphysema (Fig. S1C). The expression of cytokines and chemokines (TNF- α , IL-6, and CXCL1) increased but did not achieve statistical significance after CS exposure (Fig. S1D). CS exposure increased the level of SP-D in the serum but did not cause any significant change in the BALF (Fig. S1E). These results indicated that 6 weeks of CS exposure induced emphysema and increased mucus production and inflammatory cytokine expression in the lungs.

Enhanced airway inflammation and emphysematous changes in ozone-induced SP-D-knockout mice

To investigate the functional role of SP-D in COPD, we used CRISPR to generate sftpd-knockout (SP-D^{-/-}) mice and confirmed the absence of SP-D in both the serum and BALF (Fig. 2A). All lung function parameters (Rrs, Ers, G, and H) were significantly increased in ozone-exposed SP-D^{-/-} mice compared to wild-type mice (Fig. 2B). Consistent with previous reports, air-exposed SP-D^{-/-} mice exhibited larger alveolar spaces in the lung, as indicated by the increased MLI compared to that of wild-type mice (Fig. 2C). Ozone exposure further enhanced the development of emphysema and the infiltration of inflammatory cells, particularly neutrophils, in the lungs of SP-D^{-/-} mice (Fig. 2D). The total number of cells and neutrophils significantly increased in the BALF of SP-D^{-/-} mice exposed to ozone compared to that of air-treated SP-D-deficient mice and wild-type mice (Fig. 2E). Moreover, the BALF of SP-D^{-/-} mice had a higher number of stained lipid-laden FMs (Fig. 2F). Air-exposed SP-D^{-/-} mice exhibited significantly increased CXCL1 levels in BALF compared to air-exposed wild-type mice. In addition, ozone exposure significantly increased the levels of IL-6 and CXCL1 in the BALF of SP-D^{-/-} mice compared to wild-type mice (Fig. 2G), which suggested that SP-D depletion promoted airway inflammation and emphysematous changes in the lungs of ozone-exposed mice.

Exogenous SP-D improved lung function and attenuated airway inflammation in ozone-exposed mice

Native SP-D (25 μ g) purified from amniotic fluid was intratracheally administered to ozone-exposed mice once per week for 3 weeks. Exogenous SP-D significantly improved lung function, as demonstrated by reductions in Rrs, Ers, G, and H, compared with those in untreated mice (Fig. 3A). SP-D alleviated inflammation in the alveoli and airways of ozone-exposed mice (Fig. 3B), reduced lung emphysema (as shown by the lower MLI (Fig. 3C)), and decreased inflammatory cell infiltration, particularly that of macrophages and neutrophils, in the BALF of SP-D-treated ozone-exposed mice (Fig. 3D). In addition, exogenous administration of native human SP-D significantly increased the levels of SP-D in the BALF but not the sera of treated mice (Fig. 3E). TNF- α , IL-6, and CXCL1 levels were significantly decreased in BALF after SP-D treatment (Fig. 3F). These data support the hypothesis that SP-D protects against airway inflammation and emphysematous changes associated with COPD.

SP-D decreased ROS production by upregulating Nrf2 and prevented ROS-induced early apoptosis of epithelial cells

Figure 4 shows that SP-D deficiency increases the level of ROS in the lungs of ozone- and CS-exposed SP-D-knockout or wild-type mice. Ex vivo bioluminescence imaging showed that SP-D^{-/-} mice

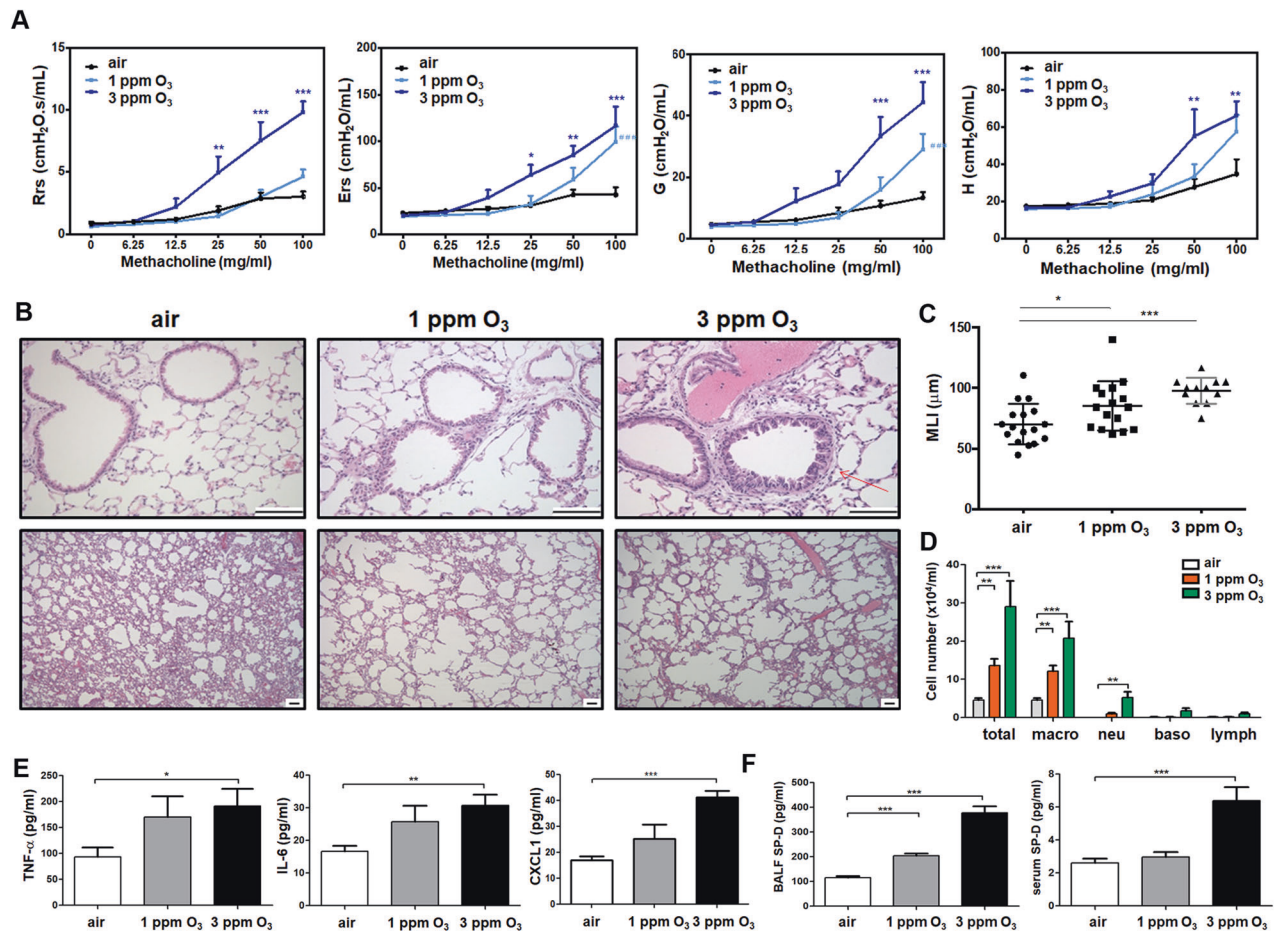


Fig. 1 Ozone induced lung inflammation and increased the level of SP-D in serum and BALF. **A** BALB/c female mice were exposed to 1 and 3 ppm ozone for 3 h 3 times per week. After exposure, lung function was determined using Snapshot150 perturbation on a FlexiVent (SCIREQ). The data represent the mean \pm SEM. * $p < 0.05$, ** $p < 0.01$, *** $p < 0.001$, two-way ANOVA vs. the air group. **B** H&E staining of lung sections. Scale bar = 100 μ m. **C** Alveolar well length was measured by the MLI. **D** BALF cell counts included total cells, macrophages (macro), neutrophils (neu), basophils (baso), and lymphocytes (lymph). The data represent the mean \pm SEM. ** $p \leq 0.01$; *** $p \leq 0.001$, Student's unpaired t test. The levels of **E** TNF- α , IL-6 and CXCL1 in the BALF and **F** SP-D in serum and BALF were measured by ELISA. The data represent the mean \pm SEM. * $p < 0.05$, ** $p \leq 0.01$, *** $p \leq 0.001$, Student's unpaired t test

had high ROS levels in their lungs under air-, ozone-, and CS-exposed conditions compared to wild-type mice, indicating that SP-D was essential for preventing ROS production in the lung (Fig. 4A). In vitro studies on cell lines also showed that pretreatment with SP-D reduced ROS production in A549 and BEAS-2B cells stimulated with 10 μ M H₂O₂ and dose-dependently reduced ROS levels in SP-D-pretreated, H₂O₂-stimulated bone marrow-derived macrophages (BMDMs) (Fig. 4B). To examine whether SP-D reduced hydrogen peroxide-induced programmed cell death, A549 cells were pretreated with 1 μ g/ml SP-D for 5 h followed by 10 μ M H₂O₂, and early-stage apoptosis was assessed (annexin V⁺ and PI⁻) by flow cytometry. H₂O₂ increased the annexin V⁺ and PI⁻ populations of A549 and BEAS-2B cells, while SP-D pretreatment significantly decreased the annexin V⁺ and PI⁻ populations of A549 cells but not BEAS-2B cells (Fig. 4C, D).

Nuclear factor erythroid 2-related Factor 2 (Nrf2) is a basic leucine zipper (bZIP) protein that can regulate the expression of antioxidant proteins that protect against oxidative damage triggered by injury and inflammation [20]. To examine whether SP-D decreased ROS production through Nrf2, A549 cells were pretreated with various doses of SP-D and then stimulated with H₂O₂. We found that pretreatment with 5 and 10 μ g/ml SP-D increased the expression of Nrf2 (Fig. 4E). In ozone-exposed (3 ppm) wild-type mice, Nrf2 protein expression in the lung was lower than that in air-exposed mice (Fig. 4F). Air-exposed SP-D^{-/-} mice exhibited lower Nrf2 protein

expression in the lung than wild-type mice. Ozone exposure significantly reduced Nrf2 expression in SP-D^{-/-} mice (Fig. 4G). The histochemistry results showed that exogenous administration of SP-D increased the expression of Nrf2 in the lungs of ozone-exposed mice compared to untreated mice (Fig. 4H).

SP-D upregulated oxidative and lipid metabolism gene expression in CS extract-treated BMDMs

To clarify the oxidative stress-related genes that are regulated by SP-D, we performed RNA-seq analysis on BMDMs treated with the medium, SP-D, CS extract, or SP-D plus CS extract. The heatmap showed significantly different expression profiles in the SP-D plus CS extract and CS only groups (Fig. S2A). Each type of treatment was widely separated in the principal component analysis (PCA) (Fig. S2B). SP-D plus CS extract changed 21 genes compared with CS alone (Fig. 4I). Several genes with significantly different expression levels in the SP-D plus CS group relative to the CS group were involved in the regulation of oxygen species metabolic processes and inflammatory responses (Fig. S2C). CS extract-treated BMDMs had 8 increased and 2 decreased genes associated with ROS metabolic processes compared with the medium control (Fig. 4J left). However, SP-D pretreatment reversed 3 of the effects of CS-inhibition, including those on formyl peptide receptor 2 (*Fpr2*), aconitate decarboxylase 1 (*Acod1*, also called *Irg-1*), and arginosuccinate synthetase 1 (*Ass1*) (Fig. 4J right).

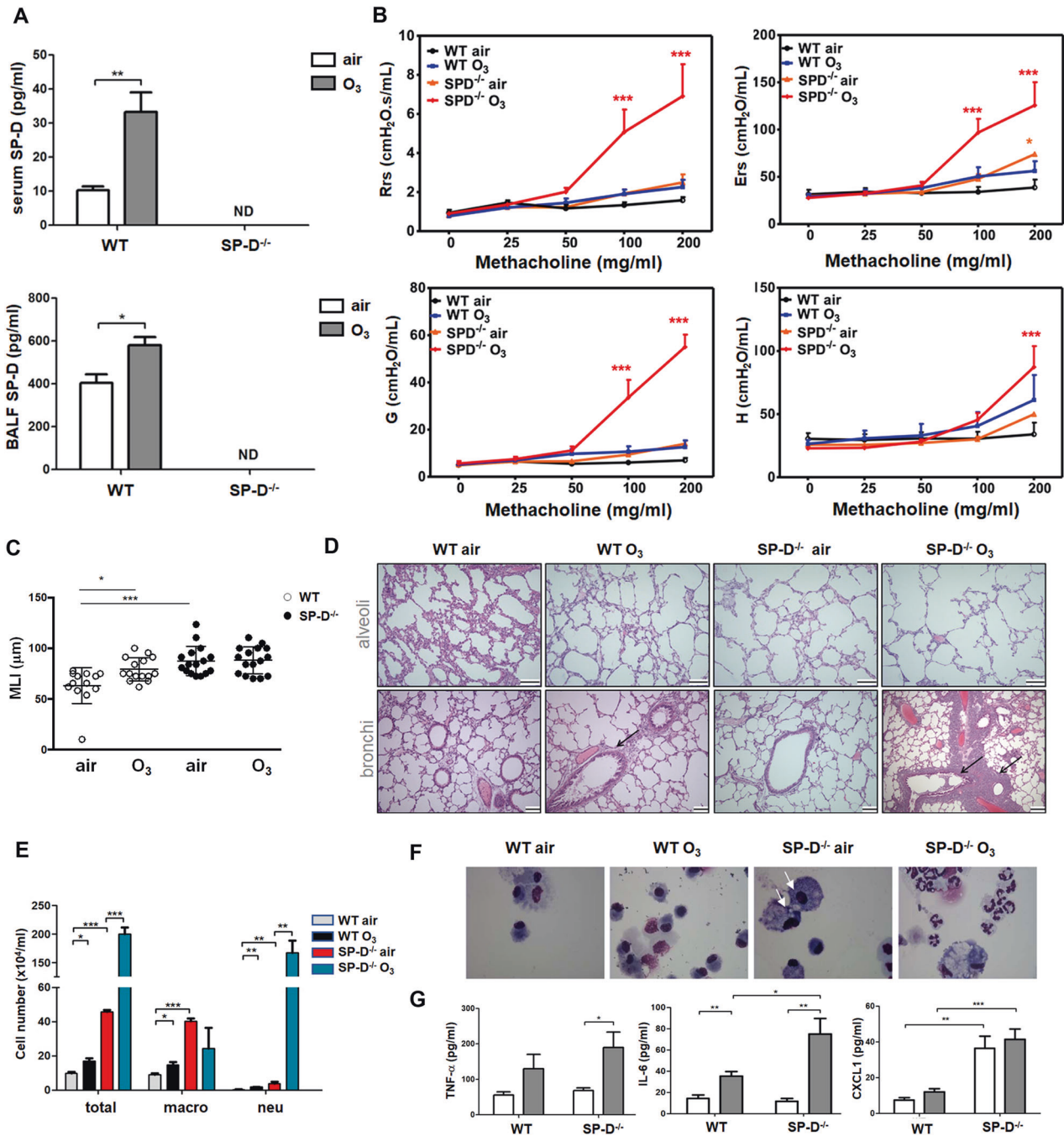


Fig. 2 Depletion of SP-D exacerbated lung inflammation in ozone-exposed mice. In ozone-exposed C57BL/6J female mice, **A** the levels of SP-D in serum and BALF were measured by ELISA. **B** Lung function was determined using Snapshot150 perturbation on FlexiVent (SCIREQ). The data represent the mean \pm SEM. * $p < 0.05$, ** $p < 0.01$, *** $p < 0.001$, two-way ANOVA vs. the air group. **C** Alveolar well length was measured by the MLI. **D** H&E staining of lung sections. **E** BALF cell counts included total cells, macrophages (macro), neutrophils (neu), basophils (baso), and lymphocytes (lymph). The data represent the mean \pm SEM. ** $p \leq 0.01$, *** $p \leq 0.001$, Student's unpaired *t* test. **F** Cells in BALF were stained with Liu and observed by light microscopy. Scale bar = 100 μ m. **G** The levels of TNF- α , IL-6, and CXCL1 were measured by ELISA. The data represent the mean \pm SEM. * $p < 0.05$, ** $p \leq 0.01$, *** $p \leq 0.001$, Student's unpaired *t* test

Increased FMs in patients with COPD and SP-D deficient mice

Our COPD patient cohort demonstrated that not only COPD patients but also smokers (both current and ex-smokers) had significantly increased oil-red-O-stained, lipid-laden FMs in BALF compared to nonsmokers (Fig. 5A–C). In ozone-induced COPD, SP-D^{-/-} mice exhibited more FMs than wild-type mice (Fig. 5D). In vitro, oxLDL-treated BMDMs exhibited more FMs than nonoxidized LDL- or LPS-treated BMDMs. Moreover, SP-D pretreatment of BMDMs decreased the number of oxLDL-induced FMs (Fig. 5E).

FM induced airway inflammation in naïve mice

We conducted adoptive transfer experiments to investigate whether FMs induced inflammation in the lung. Naïve mice were adoptively transferred medium-, LDL-, and oxLDL-treated BMDMs on Day 0. The mice were then intratracheally administered PBS or LPS on Day 2 (Fig. S3A). OxLDL-treated BMDMs significantly induced cell infiltration and IL-1 β and TNF- α production in the lungs of LPS-treated mice but not PBS-treated mice (Fig. S3B, C). In LPS-treated mice, oxLDL-treated BMDMs resulted in higher small

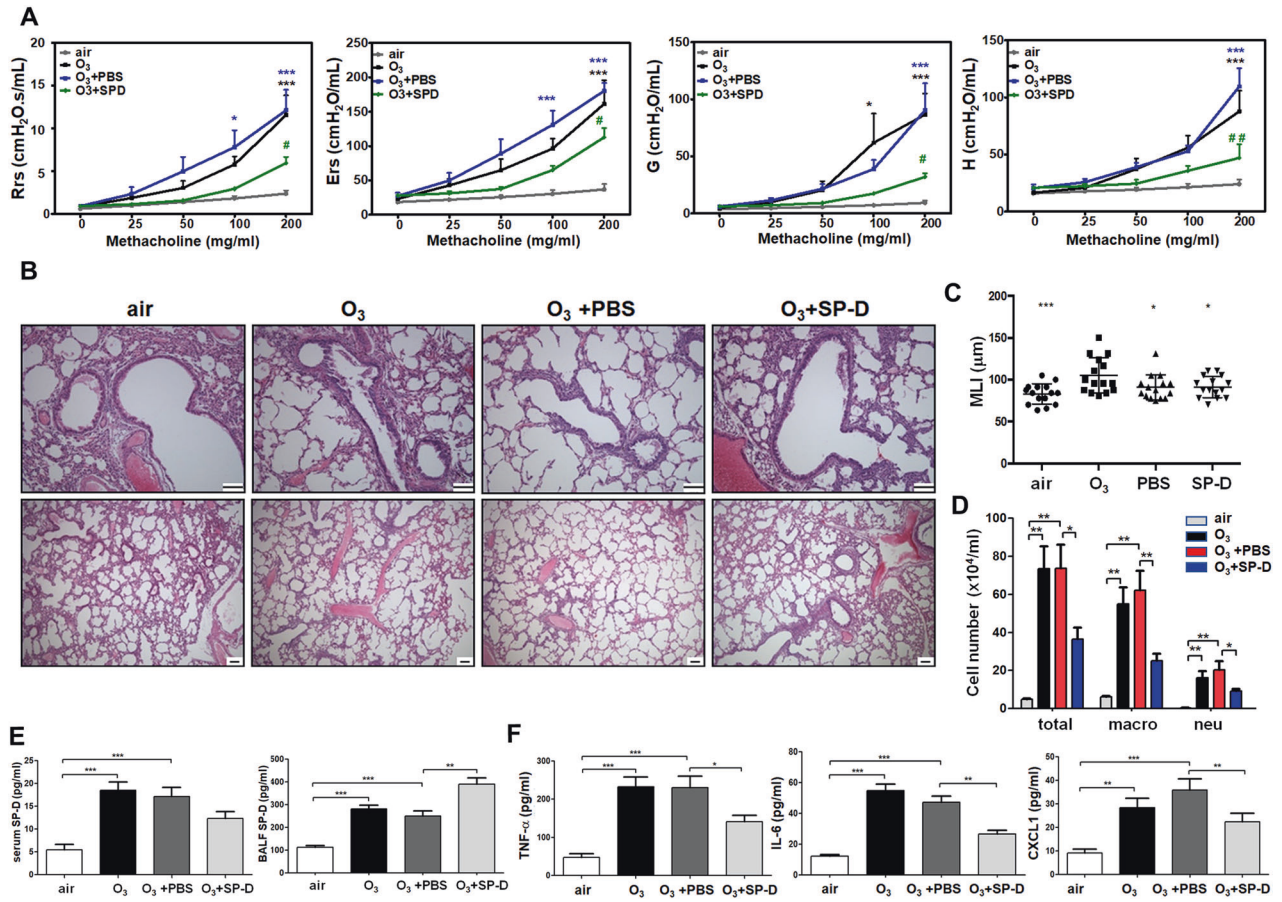


Fig. 3 Exogenous SP-D alleviated lung function and inflammation and reduced cell infiltration. **A** Ozone-exposed BALB/c female mice were treated with SP-D or PBS once per week, and lung function was determined using Snapshot150 perturbation on a FlexiVent (SCIREQ). The data represent the mean \pm SEM. * $p < 0.05$, ** $p < 0.01$, *** $p < 0.001$, two-way ANOVA vs. the air group. **B** H&E staining of lung sections. Scale bar = 100 μ m. **C** Alveolar well length was measured by the MLI. **D** BALF cell counts included total cells, macrophages (macro), neutrophils (neu), basophils (baso), and lymphocytes (lymph). The data represent the mean \pm SEM. ** $p \leq 0.01$; *** $p \leq 0.001$, Student's unpaired *t* test. **E** The levels of SP-D in serum and BALF. **F** TNF- α , IL-6, and CXCL1 were measured by ELISA. The data represent the mean \pm SEM. * $p < 0.05$, *** $p \leq 0.001$, Student's unpaired *t* test

airway thickness than that in control mice (Fig. S3D). After confirming that oxLDL-treated BMDMs induced more severe inflammation in LPS-treated mice, we examined whether rhSP-D-pretreated FMs reduced inflammation in the LPS treatment model (Fig. S3E). Mice that received SP-D plus oxLDL-treated BMDMs had significantly reduced total cell numbers (Fig. S3F), levels of TNF- α (Fig. S3G), and percentages of total foamy cells (Fig. S3H, I) and alleviation of the thickened trachea (Fig. S3J) in the lungs compared to those in the oxLDL-treated BMDM groups.

SP-D inhibited FM-induced impaired lung function and airway inflammation in mice with ozone-induced COPD

Next, we examined the effect of exogenous FM administration on an ozone-induced mouse model of COPD. BMDMs were treated with the medium (BM), LDL (BML), and oxLDL (BMO) for 1 day, and then intratracheal adoptive transfer with BMDMs was performed into the lungs of ozone-exposed mice, as shown in the protocol (Fig. 5F). Impaired lung function was further exacerbated in ozone-exposed mice in the BMO (O-BMO) group (Fig. 5G). These mice had higher mucus accumulation in their airways compared to those in the other treatment groups (Fig. 5H). However, no differences were found in inflammatory cell infiltration among the ozone-exposed groups (Fig. 5I). These data suggest that FMs enhance ozone-induced airway inflammation in the lung.

To investigate whether SP-D inhibited FM-induced lung inflammation in ozone-exposed COPD mice, BMDMs were first pretreated with

SP-D and stimulated with oxLDL (SP-D-BMO) and then adoptively transferred into ozone-exposed mice (Fig. 6A). SP-D-BMO alleviated the impaired lung function (Fig. 6B) and reduced cell infiltration (Fig. 6C) and mucus production in the airways (Fig. 6D) of recipient mice compared to those that received only oxLDL-treated BMDMs (BMO). To mimic the severe acute exacerbation of COPD in mice during bacterial infections, we first administered low-dose (10 μ g/ml) LPS intratracheally and then subjected the mice to chronic ozone exposure for 7 days (Fig. 6E). Although mice treated with SP-D-BMO exhibited no differences in respiratory mechanics compared to those in the other groups (Fig. 6F), SP-D-BMO significantly decreased the total infiltrated cells (Fig. 6G) and the percentage of FMs (Fig. 6H, I) and reduced the production of CXCL1, IL-1 β , TNF- α and IL-6 (Fig. 6J) in the BALF of recipient mice compared to the mice that received only oxLDL-treated BMDMs. Mice treated with SP-D-BMO showed significantly reduced inflammatory cell infiltration in airways and alveoli (Fig. 6K). These data suggest that SP-D may improve impaired lung function and inflammation in COPD by reversing the pathogenesis of FMs.

SP-D modified gene expression in oxLDL-treated BMDMs

To investigate how SP-D regulates the inflammatory function and gene expression of FMs, we analyzed the levels of ROS, cytokines, and RNA expression in LDL-, oxidized LDL-, oxidized LDL plus SP-D-, and SP-D-treated BMDMs. Oxidized LDL-treated BMDMs had higher levels of ROS than medium- or LDL-treated BMDMs. SP-D reduced the ROS

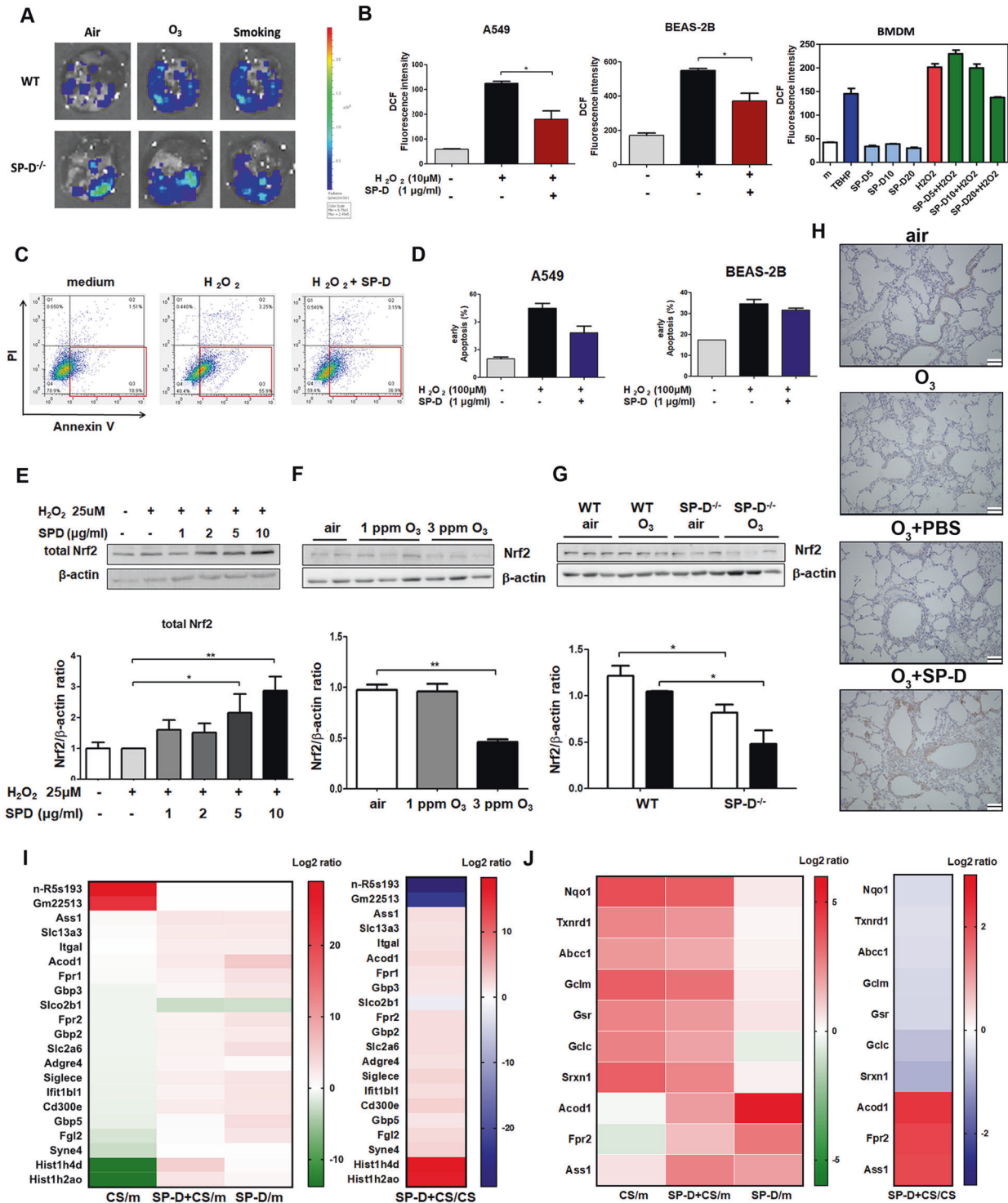


Fig. 4 SP-D pretreatment decreased ROS production and early-stage apoptotic cells and induced the expression of Nrf2. **A** Bioluminescence imaging of ROS production in the lungs of air-, ozone-, and cigarette smoke-exposed COPD C57BL/6J female mice was performed with an L-012 luminescent probe (IVIS Lumina LT Series III, PerkinElmer, USA). **B** A549, BEAS-2B cells, and BMDMs were pretreated with SP-D followed by H₂O₂. ROS production was examined by DCFDA. **C** Early-stage apoptosis (annexin V⁺ and PI⁺) in A549 and BEAS-2B cells was measured by flow cytometry. **D** Percentage of cells in early apoptosis (A549 and BEAS-2B). **E** A549 cells were pretreated with 1, 2, 5, or 10 μg/ml SP-D and then treated with H₂O₂. Nrf2 protein expression was examined by western blotting. SP-D pretreatment yielded a dose-dependent increase in Nrf2 expression. Nrf2 expression in the lung tissues of **F** wild-type and **G** SP-D^{-/-} mice was examined by western blotting. **H** After SP-D administration, Nrf2 expression in the lung tissue was examined by IHC. Scale bar = 100 μm. BMDMs were treated with medium (m), recombinant full length-SP-D (SP-D), and cigarette extract (CS) or were pretreated with SP-D and then treated with cigarette extract (SP-D + CS). **I** In a two-fold-change analysis, SP-D + CS regulated the expression of 21 genes compared with CS. **J** Gene heatmap of log₂-transformed ratios of oxidative stress gene expression. The left gene heatmap shows the log₂ ratios of CS, SP-D + CS, and SP-D treatment normalized to the medium control (CS/m, SP-D + CS/m, and SP-D/m). The right gene heatmap shows the log₂ ratios of SP-D + CS normalized to CS (SP-D + CS/CS)

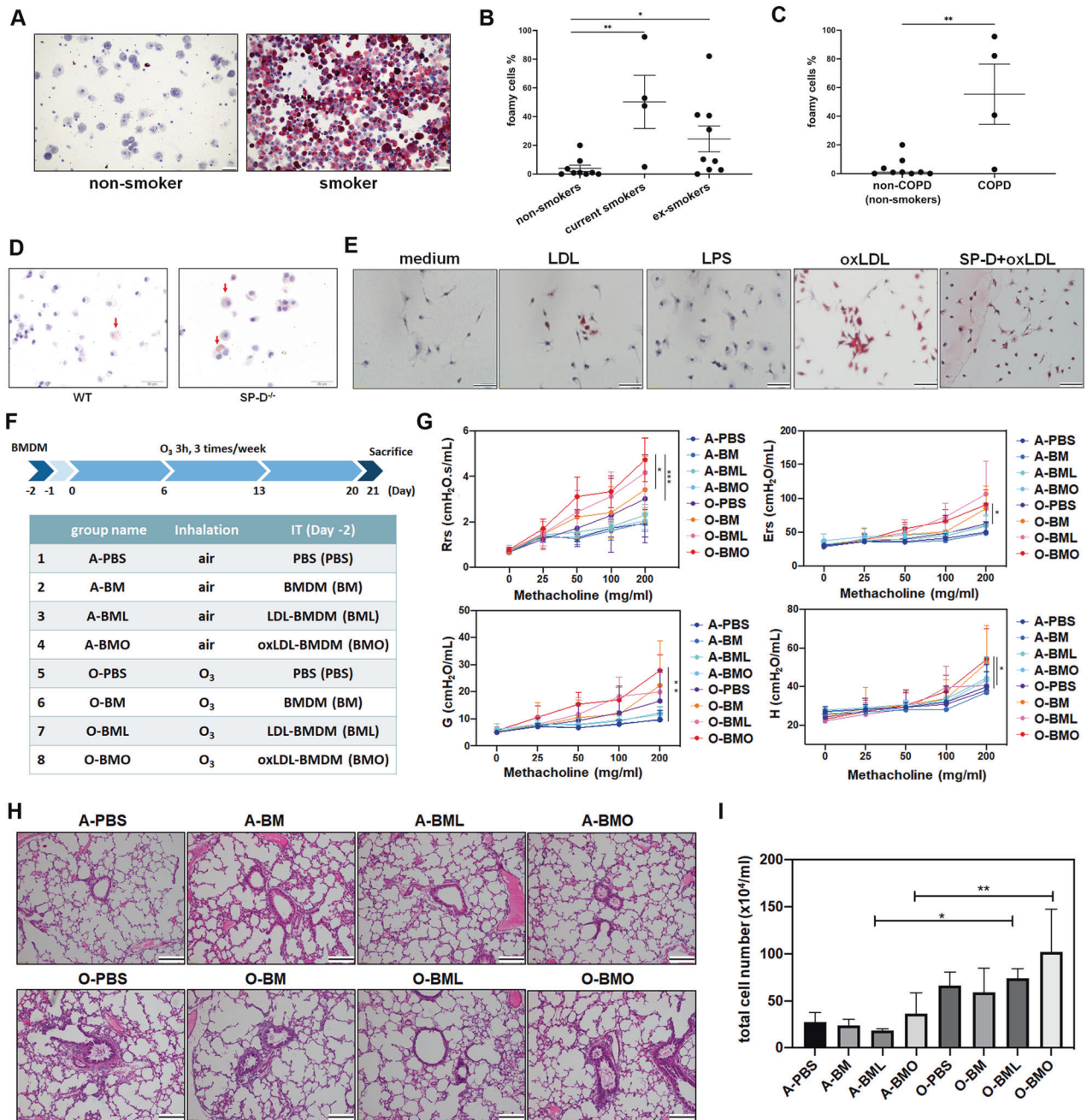


Fig. 5 Foamy cells were significantly increased in smokers, and COPD and ozone-exposed mice with oxLDL-treated BMDMs exhibited increased inflammation in the lung. **A** Foamy cells in BALF were stained with oil red O. The percentage of foamy cells was calculated in **B** never-smokers and non-COPD controls ($n = 9$). Smokers included current smokers ($n = 4$), ex-smokers ($n = 9$), and **C** smokers with COPD ($n = 4$). The data represent the mean \pm SEM. $*p < 0.05$, $**p < 0.01$, Student's unpaired t test vs. controls. Scale bar = 50 μ m. **D** Ozone-induced foamy macrophages in C57BL/6J female wild-type and SP-D^{-/-} female mice. Foamy macrophages were examined by oil red O staining. **E** BMDMs were pretreated with or without SP-D and then treated with LPS, LDL, and oxLDL. Foamy cells were examined by staining with oil red O. Scale bar = 50 μ m. **F** C57BL/6J female mice received PBS only (PBS), medium, or LDL- or oxLDL-treated BMDMs (BM, BML, and BMO) in the air- (A-PBS, A-BM, A-BML, and A-BMO) or ozone- (O-PBS, O-BM, O-BML, and O-BMO) exposed mouse model. **G** Lung function was determined using Snapshot150 perturbation on a FlexiVent (SCIREQ). The data represent the mean \pm SEM. $*p < 0.05$, $**p < 0.01$, $***p < 0.001$, two-way ANOVA vs. the air group. **H** H&E staining of lung sections. Scale bar = 50 μ m. **I** Number of total cells in BALF

production of oxLDL-treated BMDMs in a dose-dependent manner (Fig. 7A). Moreover, oxLDL-treated BMDMs had increased expression of CXCL1, CCL2, and IL-6, whereas pretreatment with SP-D reduced the expression of CXCL1 and CCL2 in oxLDL-treated BMDMs (Fig. 7B). The RNA-seq and PCA results showed that the gene expression profile can be clearly divided into three clusters: medium (M) and LDL treatment (LDL); oxLDL treatment (oxLDL) and SP-D plus oxLDL treatment (SP-

D + oxLDL); and SP-D treatment (SP-D) (Fig. S4A, B). OxLDL was shown to regulate the expression of genes involved in several biological processes, such as the response to oxidative stress, inflammation, and toxic substances (Fig. S4C). We found that oxLDL increased the level of oxidative stress- (Fig. 7C) and cytokine activity (Fig. 7D)-related genes, while SP-D pretreatment reversed this oxLDL-induced upregulation. SP-D pretreatment also reduced the expression of several genes

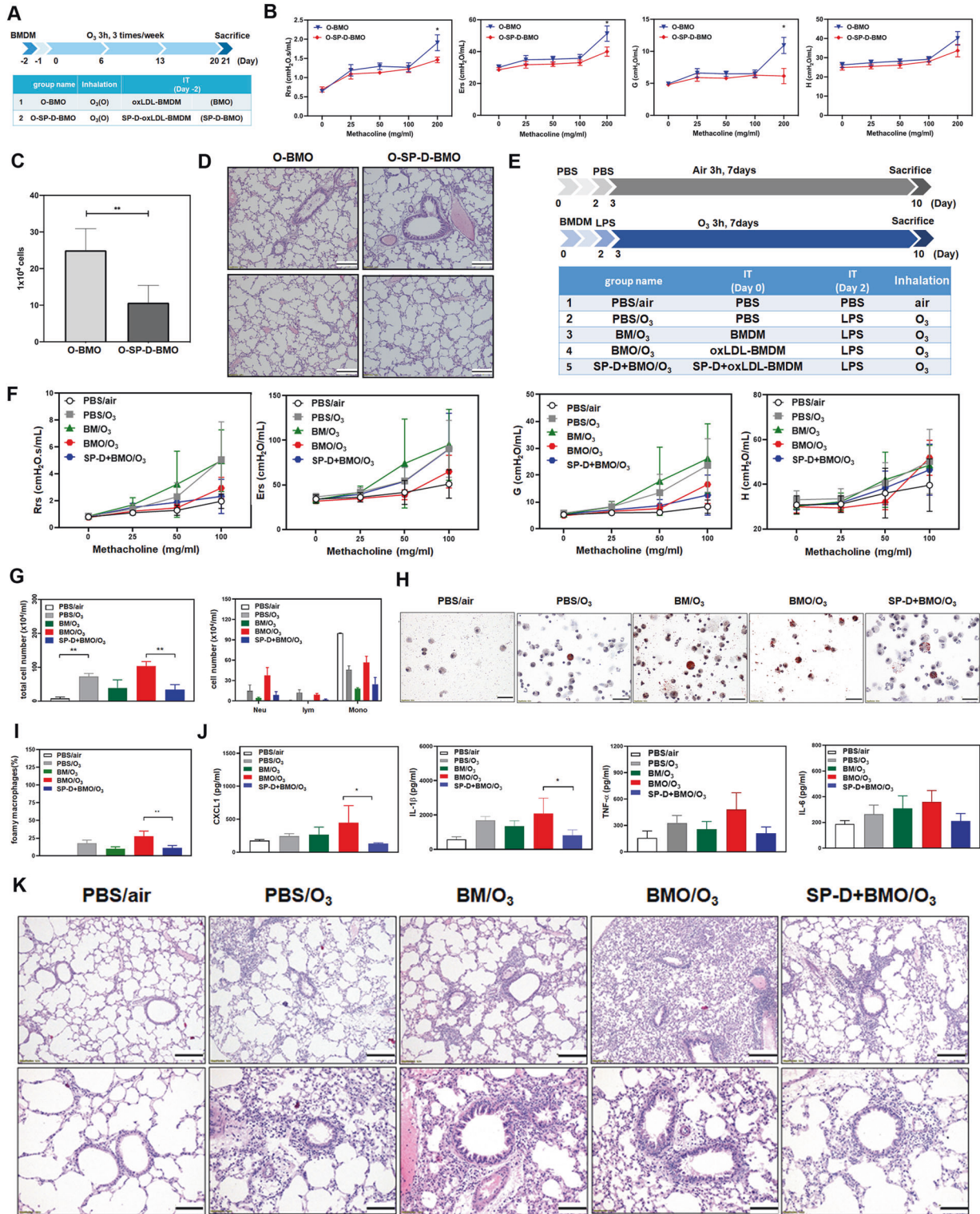


Fig. 6 SP-D combined with oxLDL alleviated airway inflammation and improved lung function in ozone-exposed mice. **A** Protocol of adoptive transfer of BMDMs in an ozone-induced C57BL/6J female mouse model of COPD. Bone marrow-derived macrophages (BMDMs) were pretreated with or without SP-D (10 μ g/ml) for 6 h and then treated with 50 μ g/ml LDL or 50 μ g/ml oxLDL for 1 day. The mice received 2×10^5 live cells by intratracheal administration. **B** Lung function was determined using Snapshot150 perturbation on FlexiVent (SCIREQ). Two-way ANOVA was performed to compare Rrs (1.46 vs. 1.91), Ers (40.00 vs. 51.27), G (10.92 vs. 6.14), and H (40.07 vs. 33.68) in the groups of mice that received oxLDL-induced foamy macrophages pretreated with SP-D (O-SP-D-BMO) vs. the group of mice that received oxLDL-induced foamy macrophages without SP-D treatment (O-BMO) during 200 mg/ml methacholine challenge. The data represent the mean \pm SEM. * $p < 0.05$. **C** Total cell numbers in BALF. **D** H&E staining of lung sections. Scale bar = 50 μ m. **E** Protocol of BMDM treatment during LPS plus ozone exposure. **F** Lung function was determined as described above. **G** Total cell numbers in BALF. **H** Foamy macrophages were stained with oil red O and then **I** quantified. **J** The levels of CXCL1, IL-1 β , TNF- α , and IL-6 were measured by ELISA. The data represent the mean \pm SEM. **K** H&E staining of lung sections. Scale bar = 100 (upper) and 200 (lower) μ m

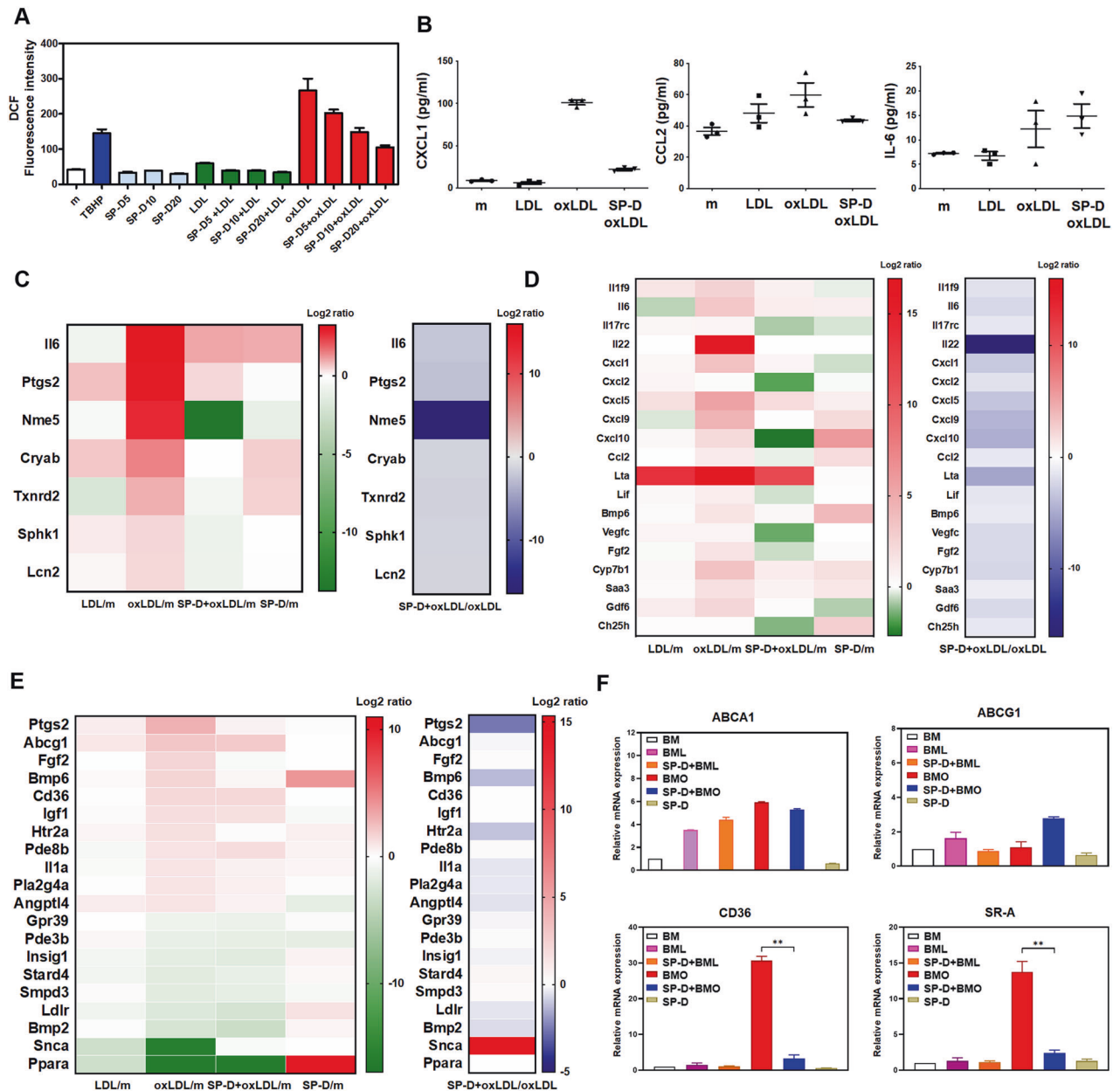


Fig. 7 SP-D reduced oxLDL-induced ROS production and CXCL1 expression, as well as the metabolism of several lipids, oxidative stress, and the regulation of inflammatory gene expression. **A** BMDMs were pretreated with 5, 10, or 20 $\mu\text{g/ml}$ SP-D, followed by treatment with 50 $\mu\text{g/ml}$ LDL or oxLDL. ROS production was examined by DCFDA. **B** BMDMs were pretreated with SP-D for 1 day and then washed 3 times with PBS. Then, the cells were treated with LDL or oxLDL for 1 day. The supernatant was collected, and the production of CXCL1, CCL2, and IL-6 was measured by ELISA. RNA expression was analyzed by RNA-seq. The left gene heatmap shows the log₂ ratios of LDL, oxLDL, SP-D + oxLDL and SP-D groups normalized to the medium control (LDL/m, oxLDL/m, SP-D + oxLDL/m, and SP-D/m). The right gene heatmap shows the log₂ ratios of SP-D + oxLDL treatment normalized to oxLDL treatment (SP-D + oxLDL/oxLDL). The genes independently regulate **C** oxidative stress, **D** cytokine activity, and **E** lipid metabolic processes. **F** The RNA expression levels of *ABCA1*, *ABCG1*, *CD36*, and *SR-A* were assessed by real-time quantitative PCR (qPCR) and normalized to *GAPDH*. The results are expressed as the mean fold change compared to the medium

involved in lipid metabolism and significantly increased the expression of alpha-synuclein (*SNCA*), which mediates lipid transport in the brain (Fig. 7E). Moreover, SP-D pretreatment significantly decreased the RNA expression of the lipid uptake receptors CD36 and SR-A compared to that in oxLDL-treated BMDMs (Fig. 7F). These findings suggested that SP-D could reduce FM formation by mediating lipid metabolism.

DISCUSSION

We explored various mechanisms by which SP-D can treat ozone- and CS-induced airway inflammation and emphysematous

destruction using experimental models of COPD. We found increased levels of SP-D in the BALF and sera of ozone- and CS-exposed mice. SP-D-knockout mice were susceptible to the accumulation of lipid-laden FMs and macrophage-rich airway inflammation caused by ozone. Importantly, exogenous rhSP-D treatment prevented the formation of oxLDL-induced FMs in vitro and reversed the airway inflammation and emphysematous changes caused by oxidative stress in vivo. Finally, we showed that SP-D upregulated genes in BMDMs that counter oxidative stress and lipid metabolism perturbations induced by CS and oxidized cholesterols. Our results showed the crucial roles of SP-D

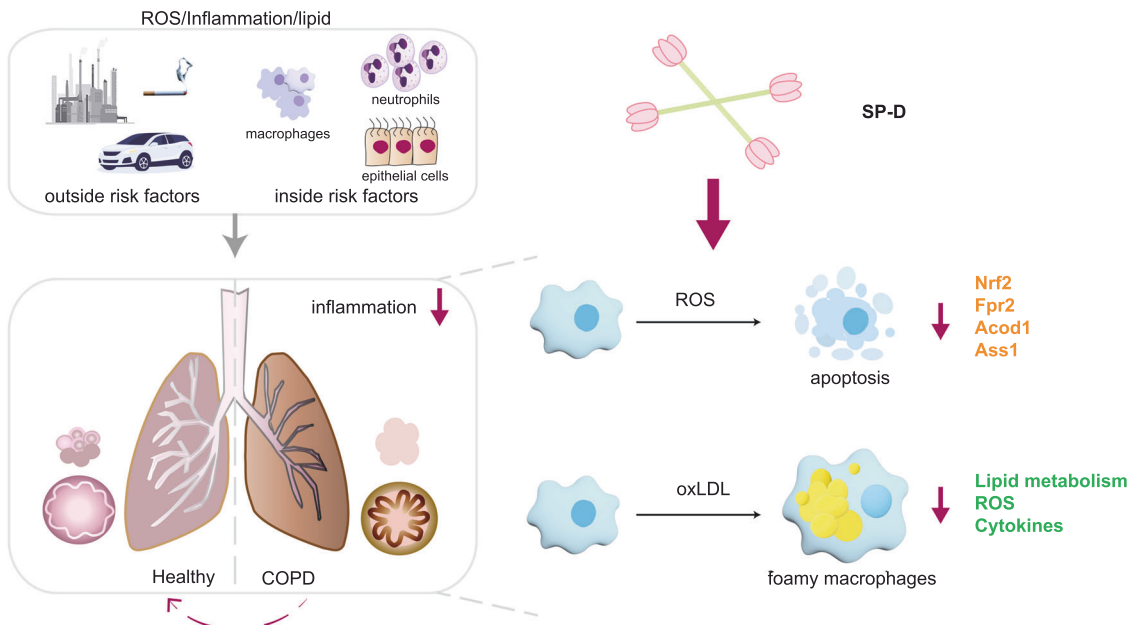


Fig. 8 Surfactant protein D inhibits lipid-laden foamy macrophages and lung inflammation in chronic obstructive pulmonary disease. SP-D deficiency exacerbates airway inflammation, lipid-laden macrophage accumulation, and emphysematous alveolar destruction in ozone- and CS-exposed lungs. Local instillation of a recombinant fragment of human surfactant protein D (rhSP-D) alleviates oxidative stress and CS-induced airway inflammation, decreases FM formation, and causes emphysematous changes in recipient mice. The biological benefits of SP-D in ozone- and CS-induced COPD may be caused by the inhibitory effect of SP-D on ROS production in dysfunctional AMs and the restoration of lipid metabolism and cellular machinery of reverse lipid transport in lipid-laden FMs

in the immunometabolism of AMs and the restoration of lipid homeostasis disrupted by ozone and CS exposure in COPD.

Although the pathogenesis of COPD is not yet fully understood, chronic exposure to oxidative stress and CS are the most common environmental factors that cause airway inflammation and alveolar structural changes in COPD. Many studies have shown the significant role of lipid metabolism disorders in COPD progression [21]. Normal lipid metabolism is important for normal lung function. Disturbances caused by smoking and oxidative stress may exacerbate the pathogenesis of COPD [22]. In fact, increased markers of oxidized lipids have been reported in the airways of patients with COPD [23, 24], including ex-smokers [25]. Lipid metabolism disorders in patients with COPD have multifaceted mechanisms, which are associated with lipid peroxidation and defects in lipid synthesis and transport [26]. The transport of lipids, including cholesterol, involves an important structural component of lipid microdomains and a complex matrix of regulation and interactions with mucosal innate immune function via CD1b in AMs [27]. Thus, the chief role of lipid metabolism in the lungs is not only as a structural or energy substrate but also as a full-fledged participant in immune defense [28].

Numerous studies involving patients with COPD have shown that chronic exposure to ozone and CS causes rapid disruption of lipid metabolism and lipid accumulation in pulmonary macrophages and AMs [29, 30]. Using single-cell RNA-seq and computational approaches, various studies have demonstrated that both pulmonary macrophages and AMs exhibit massive transcriptional plasticity in the alveolar space with increasing invasion and proliferation of cells, the loss of MHC expression, reduced cellular motility, altered lipid metabolism, and a metabolic shift reminiscent of mitochondrial dysfunction in COPD [31]. These lipid-laden FMs release inflammatory mediators such as TNF- α and IL-1 β and, more importantly, ROS that regulate the activities of pulmonary and vascular matrix metalloproteinases in patients with COPD [13, 27]. Our study clearly showed that direct administration of oxLDL-induced FMs into the trachea induced airway inflammation in recipient mice (Fig. 5) and exacerbated

emphysematous lung changes induced by ozone exposure (Fig. 5) and LPS stimulation (Fig. S3). These findings represent strong evidence for the pathogenic role of dysfunctional AMs in COPD.

Pulmonary surfactant protein D, which is secreted by alveolar type II cells and recycled by AMs, has an essential and protective role in COPD. SP-D-depleted mice spontaneously developed emphysema-like pathology [11]. The lungs of SP-D-deficient mice showed disturbances in surfactant homeostasis and the accumulation of enlarged FMs overproducing ROS and proinflammatory factors [11]. The administration of recombinant full-length or a fragment of human SP-D could prevent or alleviate airway inflammation and emphysematous alveolar destruction in recipient mice during chronic ozone or CS exposure (Fig. 3) [32, 33].

Another important piece of evidence of the protective role of SP-D in COPD is the finding that SP-D could prevent oxLDL-induced FM formation in vitro (Fig. 5E) and that pretreatment of these FMs with SP-D could reverse the FM-induced airway inflammation and emphysematous changes in ozone-exposed recipient mice (Fig. 6). Oxidized LDL represents various modifications of both lipid and apolipoprotein B (apo B) components by lipid peroxidation during oxidative stress [12, 34]. Oxidized LDL promotes atherosclerosis and lung inflammation through inflammatory and immunologic mechanisms that cause the formation of macrophage foam cells [34, 35]. CS exposure is associated with damaged pulmonary surfactants, inflammation, and dysfunctional processing and lipid accumulation in AMs. The mechanism of this disrupted lipid metabolism in foamy AMs is not yet clear. As decreased PPAR- γ and ATP-binding cassette transporter G1 (ABCG1) levels were found in foamy AMs from pulmonary alveolar proteinosis patients and GM-CSF-knockout (KO) mice, in vivo instillation of lenti-PPAR- γ resulted in the upregulation of ABCG1 and PPAR- γ expression in GM-CSF-KO AMs. Consequently, intracellular lipid accumulation decreased and cholesterol efflux activities increased [36], suggesting that PPAR- γ and ABCG1 were involved in surfactant catabolism.

The function of SP-D in lipid metabolism was disrupted by oxidative stress, serum protease leakage into the alveolar space, and AM dysfunction caused by oxidative stress and chronic CS exposure [5].

Our results showed that SP-D inhibited ROS production- and the expression of lipid metabolism-related genes (Fig. 7). These effects were enhanced by oxLDL stimulation in BMDMs. Moreover, SP-D inhibited the RNA expression of the oxLDL-lipid uptake receptors CD36 and SR-A (Fig. 7F), which may improve the reverse cholesterol transport pathway through ABCA1 and ABCG1 upregulation and increase the mobilization of cellular cholesterol to HDL particles in the extracellular space. Although we do not present direct evidence, SP-D may function like adiponectin, which can induce ABCA1-mediated reverse cholesterol transport from macrophages via the activation of PPAR- γ and LXR α/β [37].

In summary, we showed that SP-D deficiency exacerbated airway inflammation, lipid-laden macrophage accumulation, and emphysematous alveolar destruction in ozone- and CS-exposed lungs. We also demonstrated that local instillation of rfhSP-D, a recombinant fragment of human surfactant protein D, alleviated oxidative stress and CS-induced airway inflammation, decreased FM formation, and caused emphysematous changes in recipient mice. The biological benefits of SP-D in ozone and CS-induced COPD may be due to the inhibitory effects of SP-D on ROS production by dysfunctional AMs and the restoration of lipid metabolism and cellular machinery associated with reverse lipid transport in lipid-laden FMs (Fig. 8). Thus, we identified a novel mechanism through which SP-D plays a critical and protective role in the pathogenesis of ozone- and CS-induced COPD.

MATERIALS AND METHODS

Mice

Eight-week-old female BALB/cByJNarl, C57BL/6, and SP-D mice were purchased from the National Laboratory Animal Center (Taiwan). The mice were housed in the Laboratory Animal Center of the College of Medicine National Cheng Kung University. Sftpd-knockout (SP-D^{-/-}) mice were generated by CRISPR/Cas 9 at the National Laboratory Animal Center (Tainan, Taiwan). The animal studies were approved by the University Institutional Animal Care and Use Committee (IACUC No. 106243, 109006, and 109266), National Cheng Kung University (NCKU). In the ozone-induced model, the mice were exposed to ozone (3 and 10 ppm) or air for 3 h per day, 3 times per week for 3 weeks. SP-D treatment involved intratracheal administration of 20 μ g of native SP-D once per week for 3 weeks. In the CS-induced mouse model, the mice were exposed to 6 cigarettes for 1 h, 5 times per week for 6 weeks. The animals were then sacrificed by intraperitoneal injection with 90 mg/kg b.w. pentobarbiturate and exsanguination. The mechanical properties of the lung were determined by using the Scireq Flexivent apparatus (SCIREQ, Montreal, QC, Canada). In the BMDM adoptive transfer experiment, the mice were intratracheally administered PBS (vehicle control), 4×10^5 BMDMs (3 weeks of ozone exposure) or 5×10^5 BMDMs (LPS and ozone exposure). These mice were then allowed 1 day of rest. On Day 2, the mice were treated with ozone or LPS as described above. After being sacrificed as described above, the mechanical properties of the lung were determined using the Scireq Flexivent apparatus (flexiVent; SCIREQ, Montreal, QC, Canada). The lung tissue was fixed in paraformaldehyde (Sigma–Aldrich Co., USA) for histology.

Collection of cells from BALF

BALF was collected by 2 instillations of 1 ml of cold saline into the trachea. The BALF was centrifuged at $300 \times g$ for 5 min at 4 °C. The cells were incubated with RBC lysis buffer (eBioscience). After 3 min, PBS was added, and the samples were centrifuged at $300 \times g$ for 5 min at 4 °C. Total cell counts were determined by a hemocytometer. Next, the cells were prepped with a cytospin and then Liu-stained (Tonyar Biotech, Tao Yuan, Taiwan). Immune cell types were identified by microscopy and the enumeration of 200 cells. Cells stained with oil red O (Sigma–Aldrich Co., USA) were counted to determine red-stained foam cells.

ELISA

Cytokines (TNF- α , IL-6, CXCL1, CCL2, and IL-1 β) in BALF or cell supernatants were measured by ELISA (R&D System, Minneapolis, MN, USA). SP-D levels in BALF and serum was measured by a monoclonal antibody based on the Mouse SP-D DuoSet ELISA kit (Catalog No. DY6839-05, R&D System, Minneapolis, MN, USA).

Lung histology and immunohistochemistry

H&E staining was performed according to the manufacturer's protocols (Sigma–Aldrich Co., USA). Paraffin-embedded sections were heated to 65 °C for 20 min and deparaffinized in HistoClear (3 \times 10 min). The sections were rehydrated in 100%, 95%, 90%, and 70% alcohol and water for 10 min. Next, the slides were placed in retrieval solution (Dako, Carpinteria, CA) and heated in a microwave for 15 min. After being cooled to room temperature for 30 min, immunohistochemistry was performed using an IHC kit (Dako, Carpinteria, CA) and Nrf2 antibodies (Abcam, Cambridge, United Kingdom). Images were acquired using an Olympus BX50 light microscope (Olympus, Center Valley, PA, USA) equipped with an Optronics MagnaFire digital camera (Optronics, Inc., Muskogee, OK, USA). Images of lung sections were captured and assessed for the mean linear intercept (MLI), which was calculated by dividing the total length of the lung section by the total number of intercepts with alveolar septal walls (scale bar = 100 μ m) [38].

Imaging ROS

The mice received L-012 by intraperitoneal administration. After 10 min, the mice were euthanized, and their lung tissue was examined by an IVIS Lumina LT Series III (PerkinElmer, USA).

Purification of human SP-D and expression of a recombinant fragment of human SP-D

Native SP-D was purified from pooled amniotic fluid, which was filtered through a 0.45- μ m membrane. The filtrate was incubated with maltose Sepharose at 4 °C, and SP-D protein was purified using a packed maltose Sepharose column by ÄKTA Start (GE Healthcare Life Sciences, USA) [39]. Recombinant human SP-D was produced and purified as described elsewhere [40] with minor modifications. To assess the purity, purified rfhSP-D was separated by SDS–PAGE. LPS was removed using Acrodisc units with a Mustang E Membrane (PALL Corporation, NY, USA). BMDMs were treated with recombinant full-length SP-D (R&D System, Minneapolis, MN, USA).

Collection of bronchoalveolar lavage fluid

Bronchoalveolar lavage (BAL) samples were collected from the participants at the National Cheng Kung University Hospital (IRB approval IRB: B-ER-109-016). The procedures were performed according to the recommended practice guideline procedures. A total of 9 never-smoker controls, 4 current smokers and 9 ex-smokers were recruited for the study. One current smoker and 3 ex-smokers were diagnosed with COPD by using the GOLD criteria with clinical correlations or by CT scans. After wedging in the targeted segmental bronchus, BAL of the unaffected lung was performed using a fiberoptic bronchoscope. The first was an installed aliquot that was disposed to avoid contamination of the bronchial sections. The flowing aliquots were instilled and withdrawn sequentially. Next, 1 ml of BAL was centrifuged at $300 \times g$ for 5 min at 4 °C. The cells were incubated with RBC lysis buffer (eBioscience). After 3 min, PBS was added, and the samples were centrifuged at $300 \times g$ for 5 min at 4 °C. The BAL cells were prepared on a microscope slide and further stained with Oil red O.

Cell treatment

A549 or BES-2B cells were pretreated with 1, 2, 5, and 10 μ g/ml SP-D for 5 h, followed by 25 μ M H₂O₂ for 2 h.

Western blotting

Samples were loaded on a 10% Tris-glycine polyacrylamide gel. After electrophoretic separation, the proteins were transferred to a polyvinylidene difluoride (PVDF) membrane. The blots were blocked in 5% dry milk blocking buffer and then washed. The following antibodies were used: Nrf2 (1:1000, GeneTex, USA), β -actin (1:5000, GeneTex, USA), and an anti-rabbit secondary antibody (1:10,000, GeneTex, USA). The probed blots were stained with an ECL western blotting substrate kit (PerkinElmer, USA) and detected by a UVP BioSpectrum Imaging System.

Flow cytometry

Approximately 10^6 cells were collected. Apoptotic cells were immediately assessed with a FITC Annexin V Apoptosis Detection Kit (BD Biosciences, San Jose, CA, USA) and a BD FACScan (BD Biosciences, San Jose, CA, USA).

Preparation of oxidized LDL (oxLDL)

Human LDL (Prospec) was oxidized by CuSO₄ (Sigma–Aldrich Co., USA) at 37 °C for 1 day. The oxidation was stopped by adding EDTA (Sigma–Aldrich Co., USA). The oxLDL was dialyzed in PBS for 2 h and exchanged three times. The oxLDL was filtered through a 0.22- μ m pore hydrophilic PVDF membrane (Merck Millipore, USA). The concentration of oxLDL was measured by using a Bio-Rad protein assay kit (Bio-Rad, Hercules, CA, USA).

Preparation of BMDMs

Bone marrow cells were obtained from the thigh bone and cultured in 10 ng/ml M-CSF for 1 week. The medium was renewed every 3 days. After 1 week, these cells transformed into macrophages, as described elsewhere [41]. The cells were distributed at 1×10^6 per well and treated with 50 μ g/ml LDL or 50 μ g/ml oxLDL. The cells were pretreated with or without SP-D (10 μ g/ml) for 1 day and washed with PBS before being treated with oxLDL. After 1 day, the cells were collected and washed with PBS.

RNA-seq analysis

BMDMs were pretreated with or without SP-D (10 μ g/ml) for 6 h and then washed with PBS. The cells were treated with 0.3% cigarette extract for 6 h and then collected. In the cigarette extract experiment, BMDMs were pretreated with or without SP-D (10 μ g/ml) for 6 h and then washed with PBS. The cells were treated with 0.3% CS for 6 h. In the oxLDL analysis, the BMDMs were pretreated with or without SP-D (10 μ g/ml) for 1 day and then washed with PBS. These cells were treated with oxLDL (50 μ g/ml) for 1 day and then collected. Total RNA was extracted using TRIzol reagent (Invitrogen, USA) according to the manufacturer's instructions. Purified RNA was quantified at 260 nm using an ND-1000 spectrophotometer (Nanodrop Technology, USA), and the quality was assessed using a Bioanalyzer 2100 (Agilent Technology, USA) with an RNA 6000 LabChip kit (Agilent Technology, USA). All RNA procedures were carried out according to Illumina protocols. The Agilent SureSelect Strand-Specific RNA Library Preparation Kit was used for library construction followed by AMPure XP bead (Beckman Coulter, USA) size selection. The sequence was determined using sequencing-by-synthesis technology (Illumina, USA). The sequencing data (FASTQ reads) were generated using Welgene Biotech's pipeline based on Illumina's base-calling program bcl2fastq v2.20 (<https://emea.support.illumina.com/downloads/bcl2fastq-conversion-software-v2-20.html>). The mRNA profiling-seq data generated from the treated groups were normalized to the data from the medium control. After a pairwise comparison, genes with ≥ 2 -fold up- and downregulation in each comparison were selected for analysis. Differential expression analysis was performed using cuffdiff (cufflinks v2.2.1) with genome bias detection/correction and Welgene in-house programs. The differentially expressed genes of each experiment were subjected to the enrichment test for functional assays using clusterProfiler v3.6. Genes associated with oxidative stress, inflammation, and lipid metabolism pathways were identified by analytical filters and used to further draw heatmaps using GraphPad Prism (GraphPad Software).

Real-time PCR analysis

Total RNA was isolated using TRIzol RNA Isolation Reagents (Thermo Fisher Scientific), and 1 μ g was treated with DNase I (Promega, USA) and reverse-transcribed (Promega, USA). qPCR Bio SyGreen Mix (PCR Biosystems) (PCR Biosystems, London, UK) was used to amplify ABCA-1, ABCG-1, CD36, and SR-A by qPCR using the following primers: ABCA-1 fwd: 5'-GCAGATCAAGC ATCCCAACT-3', rev: 5'-CCAGAGAATGTTTCATTGTCCA-3' [42]; ABCG-1 fwd: 5'-GGGTCTGAAGCTGCCTACTCT-3', rev: 5'-TACTCCCCTGATGCCACTTC-3' [43]; CD36 fwd: 5'-TTGTACCTATACTGTGGCTAAATGAGA-3', rev: 5'-TCTACCATGCCC AAGGAGCTT-3' [44]; SR-A fwd: 5'-GCATCCCTTCTCACAGC-3', rev: 5'-AAT GAGGGCAGCCTTGAA-3' [45]; and GAPDH fwd: 5'-GGTCATCCATGACAAC TTTGG C -3' rev: 5'-TGATGCAGGGATGATGTTCTG -3'.

Cellular ROS assay with DCFDA

A cellular ROS assay was conducted using the DCFDA/H₂DCFDA—Cellular ROS Assay Kit (Abcam, Cambridge, United Kingdom). The cells were seeded overnight on a 96-well culture plate (2.5×10^4 cells/well) with a clear flat bottom and black sides. The cells were washed with 1 \times buffer and then stained with diluted DCFDA solution for 45 min at 37 °C. The cells were then treated with different doses of H₂O₂ and 50 μ M tert-butyl hydrogen peroxide (TBHP, as a positive control) in 1 \times buffer supplemented with 10% FBS for 4 h using a measured plate in Ex/Em = 485/535 nm end-point mode using FlexStation 3 (Molecular Devices, LLC).

Statistical analysis

Cell numbers, ELISA data, and mRNA expression were analyzed by Student's unpaired t test. The response to methacholine challenge under various conditions was compared by two-way ANOVA. The mean \pm SEM are presented as a bar chart using GraphPad Prism 8. A value of $p < 0.05$ indicates statistical significance.

REFERENCES

- Barnes PJ, Burney PG, Silverman EK, Celli BR, Vestbo J, Wedzicha JA, et al. Chronic obstructive pulmonary disease. *Nat Rev Dis Prim.* 2015;1:15076.
- Cheng SL, Chan MC, Wang CC, Lin CH, Wang HC, Hsu JY, et al. COPD in Taiwan: a national epidemiology survey. *Int J Chron Obstruct Pulmon Dis.* 2015;10:2459–67.
- Sullivan J, Pravosud V, Mannino DM, Siegel K, Choate R, Sullivan T. National and state estimates of COPD morbidity and mortality—United States, 2014–2015. *Chronic Obstr Pulm Dis.* 2018;5:324–33.
- Mittal M, Siddiqui MR, Tran K, Reddy SP, Malik AB. Reactive oxygen species in inflammation and tissue injury. *Antioxid Redox Signal.* 2014;20:1126–67.
- Cañadas O, Olmeda B, Alonso A, Pérez-Gil J. Lipid-protein and protein-protein interactions in the pulmonary surfactant system and their role in lung homeostasis. *Int J Mol Sci.* 2020;21:3708.
- Knudsen L, Ochs M, Mackay R, Townsend P, Deb R, Mühlfeld C, et al. Truncated recombinant human SP-D attenuates emphysema and type II cell changes in SP-D deficient mice. *Respir Res.* 2007;8:70.
- Wright JR. Immunoregulatory functions of surfactant proteins. *Nat Rev Immunol.* 2005;5:58–68.
- Vandivier RW, Ogden CA, Fadok VA, Hoffmann PR, Brown KK, Botto M, et al. Role of surfactant proteins A, D, and C1q in the clearance of apoptotic cells in vivo and in vitro: calreticulin and CD91 as a common collectin receptor complex. *J Immunol.* 2002;169:3978–86.
- Knudsen L, Atochina-Vasserman EN, Massa CB, Birkelbach B, Guo CJ, Scott P, et al. The role of inducible nitric oxide synthase for interstitial remodeling of alveolar septa in surfactant protein D-deficient mice. *Am J Physiol Lung Cell Mol Physiol.* 2015;309:L959–69.
- Korfhagen TR, Sheftelyevich V, Burhans MS, Bruno MD, Ross GF, Wert SE, et al. Surfactant protein-D regulates surfactant phospholipid homeostasis in vivo. *J Biol Chem.* 1998;273:28438–43.
- Wert SE, Yoshida M, LeVine AM, Ikegami M, Jones T, Ross GF, et al. Increased metalloproteinase activity, oxidant production, and emphysema in surfactant protein D gene-inactivated mice. *Proc Natl Acad Sci USA.* 2000;97:5972–7.
- Levitani I, Volkov S, Subbaiah PV. Oxidized LDL: diversity, patterns of recognition, and pathophysiology. *Antioxid Redox Signal.* 2010;13:39–75.
- Hirama N, Shibata Y, Otake K, Machiya J, Wada T, Inoue S, et al. Increased surfactant protein-D and foamy macrophages in smoking-induced mouse emphysema. *Respirology.* 2007;12:191–201.
- Lian X, Yan C, Yang L, Xu Y, Du H. Lysosomal acid lipase deficiency causes respiratory inflammation and destruction in the lung. *Am J Physiol Lung Cell Mol Physiol.* 2004;286:L801–7.
- Nandy D, Sharma N, Senapati S. Systematic review and meta-analysis confirms significant contribution of surfactant protein D in chronic obstructive pulmonary disease. *Front Genet.* 2019;10:339.
- Ju CR, Liu W, Chen RC. Serum surfactant protein D: biomarker of chronic obstructive pulmonary disease. *Dis Markers.* 2012;32:281–7.
- Wang H, Li F, Huang H, Wu F, Chen L, Zhang D, et al. Serum surfactant protein D is a potential biomarker for chronic obstructive pulmonary disease: a systematic review and meta-analysis. *Clin Lab.* 2019;65. <https://doi.org/10.7754/Clin.Lab.2019.190539>.
- Obeidat M, Li X, Burgess S, Zhou G, Fishbane N, Hansel NN, et al. Surfactant protein D is a causal risk factor for COPD: results of Mendelian randomisation. *Eur Respir J.* 2017;50:1700657.
- Ou CY, Chen CZ, Hsiue TR, Lin SH, Wang JY. Genetic variants of pulmonary SP-D predict disease outcome of COPD in a Chinese population. *Respirology.* 2015;20:296–303.
- Zhu H, Jia Z, Zhang L, Yamamoto M, Misra HP, Trush MA, et al. Antioxidants and phase 2 enzymes in macrophages: regulation by Nrf2 signaling and protection against oxidative and electrophilic stress. *Exp Biol Med.* 2008;233:463–74.
- Kotlyarov S, Kotlyarova A. Molecular mechanisms of lipid metabolism disorders in infectious exacerbations of chronic obstructive pulmonary disease. *Int J Mol Sci.* 2021;22:7634.
- Azimzadeh Jamalkandi S, Mirzaie M, Jafari M, Mehrani H, Shariati P, Khodabandeh M. Signaling network of lipids as a comprehensive scaffold for omics data integration in sputum of COPD patients. *Biochim Biophys Acta.* 2015;1851:1383–93.
- Ko FW, Lau CY, Leung TF, Wong GW, Lam CW, Hui DS. Exhaled breath condensate levels of 8-isoprostane, growth related oncogene alpha and monocyte chemoattractant protein-1 in patients with chronic obstructive pulmonary disease. *Respir Med.* 2006;100:630–8.

24. Bartoli ML, Novelli F, Costa F, Malagrino L, Melosini L, Bacci E, et al. Malondialdehyde in exhaled breath condensate as a marker of oxidative stress in different pulmonary diseases. *Mediators Inflamm.* 2011;2011:891752.
25. Montuschi P, Collins JV, Ciabattini G, Lazzeri N, Corradi M, Kharitonov SA, et al. Exhaled 8-isoprostane as an in vivo biomarker of lung oxidative stress in patients with COPD and healthy smokers. *Am J Respir Crit Care Med.* 2000;162:1175–7.
26. Miró O, Alonso JR, Jarreta D, Casademont J, Urbano-Márquez A, Cardellach F. Smoking disturbs mitochondrial respiratory chain function and enhances lipid peroxidation on human circulating lymphocytes. *Carcinogenesis.* 1999;20:1331–6.
27. Ween MP, White JB, Tran HB, Mukaro V, Jones C, Macowan M, et al. The role of oxidised self-lipids and alveolar macrophage CD1b expression in COPD. *Sci Rep.* 2021;11:4106.
28. Fessler MB. A new frontier in immunometabolism. Cholesterol in Lung health and disease. *Ann Am Thorac Soc.* 2017;14:S399–405.
29. Morissette MC, Shen P, Thayaparan D, Stämpfli MR. Disruption of pulmonary lipid homeostasis drives cigarette smoke-induced lung inflammation in mice. *Eur Respir J.* 2015;46:1451–60.
30. Fujii W, Kapellos TS, Baßler K, Händler K, Holsten L, Knoll R, et al. Alveolar macrophage transcriptomic profiling in COPD shows major lipid metabolism changes. *ERJ Open Res.* 2021;7:00915-2020.
31. Baßler K, Fujii W, Kapellos TS, Horne A, Reiz B, Dudkin E, et al. Alterations of multiple alveolar macrophage states in chronic obstructive pulmonary disease. *bioRxiv.* 2020. <https://doi.org/10.1101/2020.05.28.121541>.
32. Fisher JH, Sheftelyevich V, Ho YS, Fligel S, McCormack FX, Korfhagen TR, et al. Pulmonary-specific expression of SP-D corrects pulmonary lipid accumulation in SP-D gene-targeted mice. *Am J Physiol Lung Cell Mol Physiol.* 2000;278:L365–73.
33. Pilecki B, Wulf-Johansson H, Støttrup C, Jørgensen PT, Djiadeu P, Nexøe AB, et al. Surfactant protein D deficiency aggravates cigarette smoke-induced lung inflammation by upregulation of ceramide synthesis. *Front Immunol.* 2018;9:3013.
34. Lara-Guzman OJ, Gil-Izquierdo Á, Medina S, Osorio E, Alvarez-Quintero R, Zuluaga N, et al. Oxidized LDL triggers changes in oxidative stress and inflammatory biomarkers in human macrophages. *Redox Biol.* 2018;15:1–11.
35. Matsuura E, Hughes GR, Khamashta MA. Oxidation of LDL and its clinical implications. *Autoimmun Rev.* 2008;7:558–66.
36. Malur A, Baker AD, Mccoy AJ, Wells G, Barna BP, Kavuru MS, et al. Restoration of PPARgamma reverses lipid accumulation in alveolar macrophages of GM-CSF knockout mice. *Am J Physiol Lung Cell Mol Physiol.* 2011;300:L73–80.
37. Hafiane A, Gasbarrino K, Daskalopoulou SS. The role of adiponectin in cholesterol efflux and HDL biogenesis and metabolism. *Metabolism.* 2019;100:153953.
38. Alzoubi A, Ghazwi R, Alzoubi K, Alqudah M, Kheirallah K, Khabour O, et al. Vascular endothelial growth factor receptor inhibition enhances chronic obstructive pulmonary disease picture in mice exposed to waterpipe smoke. *Folia Morphol.* 2018;77:447–55.
39. Dodagatta-Marri E, Qaseem AS, Karbani N, Tsolaki AG, Waters P, Madan T, et al. Purification of surfactant protein D (SP-D) from pooled amniotic fluid and bronchoalveolar lavage. *Methods Mol Biol.* 2014;1100:273–90.
40. Hsieh MH, Beirag N, Murugaiah V, Chou YC, Kuo WS, Kao HF, et al. Human surfactant protein D binds spike protein and acts as an entry inhibitor of SARS-CoV-2 pseudotyped viral particles. *Front Immunol.* 2021;12:641360.
41. Assouvie A, Daley-Bauer LP, Rousselet G. Growing murine bone marrow-derived macrophages. *Methods Mol Biol.* 2018;1784:29–33.
42. Hirai T, Fukui Y, Motojima K. PPARalpha agonists positively and negatively regulate the expression of several nutrient/drug transporters in mouse small intestine. *Biol Pharm Bull.* 2007;30:2185–90.
43. Kang JH, Ko HM, Han GD, Lee SY, Moon JS, Kim MS, et al. Dual role of phosphatidylserine and its receptors in osteoclastogenesis. *Cell Death Dis.* 2020;11:497.
44. Sekine S, Yao A, Hattori K, Sugawara S, Naguro I, Koike M, et al. The ablation of mitochondrial protein phosphatase Pgam5 confers resistance against metabolic stress. *EBioMedicine.* 2016;5:82–92.
45. He X, Chen X, Wang L, Wang W, Liang Q, Yi L, et al. Metformin ameliorates Ox-LDL-induced foam cell formation in raw264.7 cells by promoting ABCG1 mediated cholesterol efflux. *Life Sci.* 2019;216:67–74.

ACKNOWLEDGEMENTS

We thank the Laboratory Animal Center, College of Medicine, National Cheng Kung University and Taiwan Animal Consortium for the technical support in IVIS.

AUTHOR CONTRIBUTIONS

MHH, LSHW, and JYW developed the study concepts and aims. MHH, HYH, JCL, YSH, SDW, and WSK performed the experiments and data extraction. CWK collected the clinical BALF samples from COPD patients. MHH, WSK, HFK, and ZGL performed the data analysis. MHH, LSHW, and JYW drafted the manuscript. All authors provided important insight into data interpretation and contributed to the final version of the manuscript.

FUNDING

This work was supported by the Ministry of Science and Technology (MOST) of Taiwan (grant numbers 103-2321-B-006-030 and 104-2321-B-006-008), funding received in part from the Headquarters of University Advancement at the National Cheng Kung University, which is sponsored by the Ministry of Education in Taiwan, and a research grant (1JA8) from the Center for Allergy, Immunology, and Microbiome (A.I.M.), China Medical University Hospital, Taichung, Taiwan.

COMPETING INTERESTS

The authors declare no competing interests.

ADDITIONAL INFORMATION

Supplementary information The online version contains supplementary material available at <https://doi.org/10.1038/s41423-022-00946-2>.

Correspondence and requests for materials should be addressed to Lawrence Shih-Hsin Wu or Jiu-Yao Wang.

Reprints and permission information is available at <http://www.nature.com/reprints>

Springer Nature or its licensor (e.g. a society or other partner) holds exclusive rights to this article under a publishing agreement with the author(s) or other rightsholder(s); author self-archiving of the accepted manuscript version of this article is solely governed by the terms of such publishing agreement and applicable law.